Chinese Physics Letters

LETTER

Formal Polarization as a Quantized Bulk Invariant: Implications for Interface Phenomena

Cite as: Hongsheng Pang *et al*. 2026 *Chin. Phys. Lett.* **43** 100702

Recommended Articles

Spin-Polarized Two-Dimensional Electron Gas with Giant Rashba Splitting at the $EuTiO_3/KTaO_3(111)$ Interface under Light Illumination
Yu-Chen Zhao *et al*.
Chin. Phys. Lett. **42**, 100703 (2025)

Unexpected Ionic Contribution Driving Polarization Switching in Hexagonal Interfacial Ferroelectrics
Hao-Wen Xu, Chun-Gang Duan, and Wen-Yi Tong
Chin. Phys. Lett. , (2026)

Interplay Between Charge Ordering and Isospin Polarization in hBN-Aligned Twisted Monolayer–Bilayer Graphene
Wang Zhu, Junwei Song, Yajuan Zhao, Kenji Watanabe, Takashi Taniguchi, Haolin Wang, and Lei Wang
Chin. Phys. Lett. **43**, 080709 (2026)

Exploration of Interfacial Conductivity and Magnetism in Manganite/Cuprate Heterostructures
Bo Du *et al*.
Chin. Phys. Lett. **43**, 020710 (2026)

Nonvolatile Electrical Control of Transport Properties in Multiferroic $OsCl_2/Sc_2CO_2$ Heterostructure
Shi-Xu Wang, Shu-Xiang Qiao, Mei-Yan Ni, Xiao-Hong Zheng, Hua Hao, Hong-Yan Lu, and Ping Zhang
Chin. Phys. Lett. **42**, 080701 (2025)

Electric Field-Controlled Interfacial Polarization Coupling in van der Waals Ferroelectric Heterojunctions
Wei Li, Heng Liu, and Hualing Zeng
Chin. Phys. Lett. **42**, 057501 (2025)

A series journal of Chinese Physical Society distributed by IOP Publishing

Chinese Physics Letters

Chin. Phys. Lett. **43** 100702 (2026)

LETTER

DOI: 10.1088/0256-307X/43/10/100702
CSTR: 32039.14.0256-307X.43.10.100702

Formal Polarization as a Quantized Bulk Invariant: Implications for Interface Phenomena

Hongsheng Pang(庞鸿升)[1] and Lixin He(何力新)[1,2,3,*]

[1]Laboratory of Quantum Information, University of Science and Technology of China, Hefei 230026, China
[2]Institute of Artificial Intelligence, Hefei Comprehensive National Science Center, Hefei 230088, China
[3]Hefei National Laboratory, University of Science and Technology of China, Hefei 230088, China

[*]Corresponding author. Email: helx@ustc.edu.cn

In crystalline solids, symmetry can constrain formal polarization to discrete values. We show that this quantized formal polarization (QFP) should be understood as a symmetry-protected bulk invariant that encodes intrinsic information about a material's symmetry and electronic structure. From this viewpoint, mismatch between the QFPs of different materials or phases represents a bulk incompatibility with potentially broad physical consequences. In particular, when such materials form an interface, the QFP mismatch imposes a nontrivial compensation requirement, which may be realized through metallic states, bound charges, structural reconstructions, or other mechanisms. Through the examples of the ZnS/MgS heterostructure, the $HfZnN_2$ domain wall, and the GaAs domain wall, we demonstrate that bulk QFP provides a predictive criterion for determining whether nontrivial interfacial compensation is required, without explicitly constructing the interface or domain wall. The specific realization of this compensation, however, must be determined from explicit calculations for each material system. Our work thus elevates formal polarization from a quantity used mainly in interface electrostatics to a more general bulk principle relevant to phase compatibility and related phenomena, and suggests a route toward designing functional quantum materials through controlled quantized polarization mismatch.

Polarization is a central quantity in crystalline solids, closely tied to symmetry, electronic structure, and functional responses. Its role in ferroelectrics has traditionally been understood within the framework of Neumann's principle, which requires macroscopic properties to conform to the symmetry of the crystal point group [1]. Within this conventional picture, only ten of the thirty-two crystallographic point groups, the so-called polar groups, are compatible with a nonzero polarization, providing the standard symmetry-based classification of ferroelectrics [2–5].

Recent studies have shown that polarization in high-symmetry crystals can exhibit a quantized character beyond the conventional classification of polar materials, as exemplified by fractional quantum ferroelectricity [6–8], where polarization takes fractional multiples of the polarization quantum. Although such behavior may appear to challenge the conventional Neumann's principle, recent work has shown that it can be understood naturally within a generalized Neumann's principle that incorporates translational symmetry [8]. This broader perspective is closely connected to the modern theory of polarization in crystals.

The pioneering work of Vanderbilt and co-workers established the Berry-phase theory of polarization and showed that polarization is an intrinsic bulk property of crystalline solids [9,10]. Within this formalism, well-defined formal polarization can be assigned to all thirty-two crystallographic point groups, including centrosymmetric ones. Importantly, in high-symmetry crystal structures, symmetry constrains formal polarization to discrete values [8]. Formal polarization in such systems therefore carries quantized bulk information fixed by symmetry, rather than serving merely as an arbitrary reference quantity. However, in high-symmetry crystals it has often been treated mainly as a non-switchable reference state, while its role as a symmetry-protected bulk invariant has remained underemphasized.

A natural consequence of such quantized bulk polarization is that mismatch between the formal polarizations of different materials or phases can generate nontrivial responses at their boundary. The interfacial consequences of polarization discontinuities have been studied extensively in the literature, including in oxide heterostructures such as $LaAlO_3/SrTiO_3$ [11–18]. In particular, the works of Vanderbilt, Stengel, and collaborators established that formal polarization provides a natural framework for understanding polarization mismatch and its electrostatic consequences even in centrosymmetric, nonferroelectric materials [19,20]. These studies established an important foundation for understanding microscopic interface electrostatics and related interfacial phenomena. Building on this foundation, we focus here on the broader physical role of quantized formal polarization (QFP) as a bulk quantity and on the consequences of mismatch between such bulk states.

In this Letter, building on the pioneering works of Stengel and Vanderbilt [19,20], we propose that QFP should be viewed as a symmetry-protected bulk invariant encoding intrinsic information about a crystal's symmetry and electronic structure. From this viewpoint, different QFP values correspond to distinct bulk states, and mismatch between them represents a bulk incompatibility rather than merely a difference in polarization values. When two materials or phases with different QFPs meet, the mismatch imposes a nontrivial compensation requirement that may be realized through pronounced electronic or structural responses (Fig. 1). Importantly, this requirement follows directly from the bulk QFPs, without explicitly constructing the interface, although explicit calculations are still needed to determine its material-specific realization. In this sense, our work elevates formal polarization from a quantity used mainly in interface electrostatics to a predictive bulk principle for diagnosing phase incompatibility.

To explore the physical consequences of QFP, we study representative heterostructures and domain walls using first-principles calculations performed with ABACUS [21,22] using numerical atomic orbital basis sets [23,24]. All structural relaxations are performed using the Perdew–Burke–Ernzerhof (PBE) functional [25]. For selected systems, the electronic structures of the PBE-relaxed configurations are further evaluated using the Heyd–Scuseria–Ernzerhof (HSE) hybrid functional [26] to assess the robustness of the electronic structure results. Optimized norm-conserving Vanderbilt pseudopotentials from

Received 18 May 2026; accepted 3 September 2026; published 30 September 2026
© 2026 Chinese Physical Society and IOP Publishing Ltd. All rights, including for text and data mining, AI training, and similar technologies, are reserved.

Check for updates

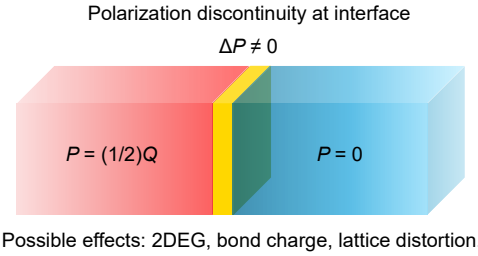

Fig. 1. Schematic showing that an interface between materials with distinct QFPs cannot be adiabatically connected, leading to polarization discontinuity and interfacial responses such as two-dimensional electron gas (2DEG) formation, bound charges, or lattice distortion.

the SG15 library [27] are employed. Electric polarization is evaluated within the modern theory of polarization [28], as implemented in PYATB [29], using tight-binding Hamiltonians constructed directly from the self-consistent ABACUS outputs. Band structures and projected density of states (PDOS) are also calculated using PYATB. Further computational details are provided in the Supplementary Materials (SM).

Representative benchmark calculations for perovskite heterostructures are provided in the SM and are consistent with the general picture discussed below. Notably, nontrivial interfacial compensation may arise even when the two constituents belong to the same QFP class. This is because formal polarization is multivalued, and a specific interface termination selects the polarization branch consistent with the corresponding bulk unit-cell cutting and layer stacking. Different terminations may therefore select different branch representatives and hence produce different branch-resolved polarization discontinuities, while leaving the underlying symmetry-protected bulk QFP classes unchanged.

We now turn to non-perovskite systems, where the predictive role of QFP mismatch can be seen more directly. As a representative example, we consider the ZnS/MgS interface, where the two constituent materials carry distinct QFPs. From the QFP viewpoint, this mismatch already signals an intrinsic interfacial incompatibility and therefore predicts a pronounced interfacial response. This is nontrivial, since both ZnS and MgS are conventionally regarded as nonpolar materials. ZnS, a typical zincblende-type compound, crystallizes in the $F\bar{4}3m$ space group with the T_d point group, whereas MgS adopts the rock-salt structure with the $Fm\bar{3}m$ space group and the O_h point group. Zincblende-type materials have long been considered unsuitable for realizing two-dimensional electron gases (2DEGs) in semiconductor heterostructures [30], which further highlights the nontrivial character of the QFP-based prediction.

We use the primitive cell throughout, under which ZnS and MgS carry distinct QFPs of 1/2 and 0, respectively [8,31]. To test the consequences of this mismatch, we construct a $(ZnS)_{10}/(MgS)_{10}$ superlattice, where the subscript denotes the number of unit cells in each constituent stacked along the c axis. ZnS and MgS have lattice constants of 5.392 Å and 5.194 Å, respectively, corresponding to a lattice mismatch of about 3.8%. The two materials share S atoms across the interface.

We now test this QFP-based prediction by fully relaxing the superlattice and computing its electronic band structure using the HSE hybrid functional, as shown in Fig. 2(a). The bulk ZnS and MgS phases are both insulating, with band gaps of 3.04 eV and 4.53 eV, respectively. Upon forming the interface, however, distinct metallic states emerge. As a control, we impose the ZnS lattice constant on bulk MgS and the MgS lattice constant on bulk ZnS. The HSE calculations for both strained bulk systems show that they remain wide-gap insulators, excluding strain-induced bulk gap closing as the origin of the interfacial metallicity.

To identify the spatial origin of the metallic bands, we perform a projected-band analysis that resolves the contributions from atoms near the interface and from those in the bulk region. As shown by the red lines in Fig. 2(a), the bands near the Fermi level are dominated by

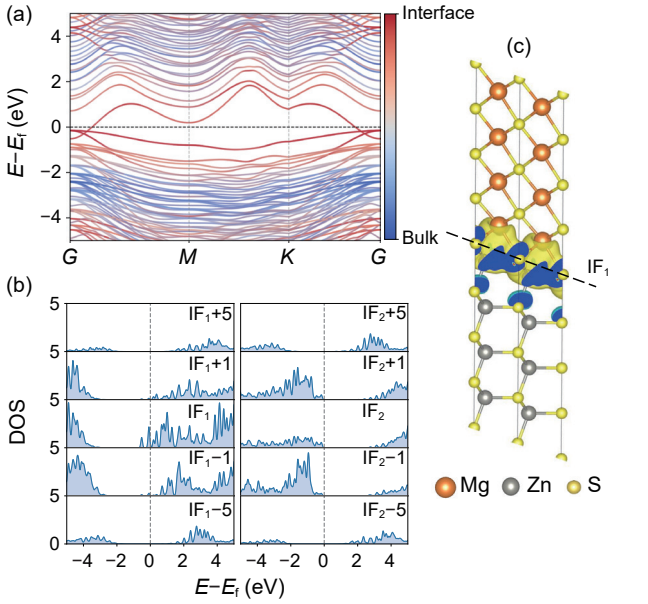

Fig. 2. (a) Band structure of the $(ZnS)_{10}/(MgS)_{10}$ superlattice, where red denotes states localized at the interfaces and blue corresponds to bulk-like states. (b) Layer-resolved PDOS for layers at different distances from IF_1 and IF_2, with metallic states emerging at IF_1. (c) Partial charge density of the metallic band near the Fermi level, showing strong electron localization at IF_1 corresponding to a 2DEG.

contributions from interfacial atoms, indicating that the metallic response is localized at the interface rather than in the bulk constituents.

Figure 2(b) shows the layer-resolved PDOS near the two interfaces, IF_1 and IF_2, whose atomic structures are presented in Fig. S4 of the SM. For each interface, the interfacial region consists of the ZnS and MgS unit cells adjacent to the junction, while IF±1 and IF±5 denote layers located one and five lattice spacings away from the interface, respectively. As shown in Fig. 2(b), the metallic states at the Fermi level arise predominantly from atoms at IF_1, whereas layers farther from the interface recover bulk-like PDOS with a large energy gap. At IF_2, interface-localized states also appear near the Fermi energy and decay rapidly away from the interface, but they do not cross the Fermi level.

Figure 2(c) shows the charge density distribution of the metallic band near the Fermi level at IF_1, corresponding to a 2DEG. The state is strongly localized at the interface, further confirming the interfacial origin of the metallic response. Its charge density is slightly shifted toward the ZnS side, consistent with the smaller bulk band gap of ZnS, which makes it more susceptible to metallic reconstruction.

Microscopically, the metallic interface states can be viewed as a response to the QFP mismatch across the boundary. The resulting polarization discontinuity leads to an electrostatic energy cost associated with the uncompensated Coulomb potential. Interfacial charge accumulation then provides an efficient way to screen this mismatch and reduce the total energy.

The interfacial phenomena observed in the ZnS/MgS superlattice illustrate a more general principle. Similar responses are found in a variety of systems, including layered nitrides and zincblende semiconductors, where QFP mismatch can be accommodated through metallic states, bound charges, or lattice reconstructions. These examples suggest that QFP mismatch provides a useful unifying framework for understanding diverse interfacial phenomena across different material classes. Additional examples are presented in the SM.

The same QFP-based principle is not restricted to heterostructures composed of different materials, but also applies to domain walls within a single material. As a representative example, $HfZnN_2$ crystallizes in the $P3m1$ space group with the C_{3v} point group. According to the generalized Neumann principle [8] and our first-principles calculations, oppositely oriented $HfZnN_2$ domains carry QFP values of

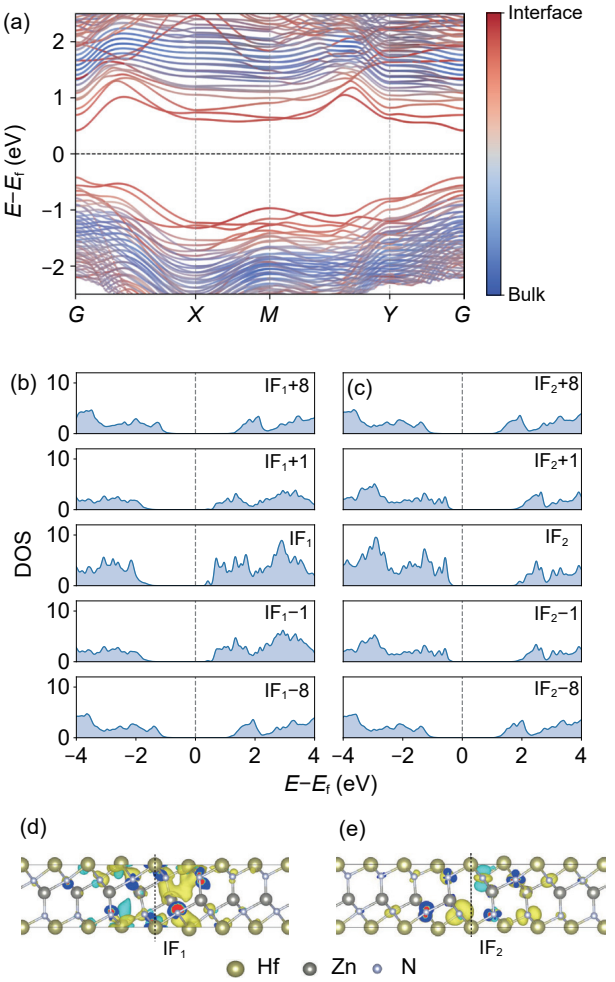

Fig. 3. (a) Band structure of the $HfZnN_2$ domain wall after structural relaxation. Red lines indicate states localized at the interfaces, while blue lines correspond to bulk-like states. (b) and (c) Layer-resolved PDOS for layers at varying distances from interfaces IF_1 and IF_2. (d) and (e) Partial charge density of the occupied band near the Fermi level, showing strong electron localization at both interfaces.

$(1/3,-1/3)$ and $(-1/3,1/3)$, respectively, producing a QFP mismatch across the domain wall. To probe the response to this mismatch, we construct a superlattice by stacking two oppositely oriented $HfZnN_2$ domains, as shown in Fig. S7 of the SM.

For the unrelaxed superlattice, the band structure and PDOS, shown in the SM, display metallic interface states crossing the Fermi level. Projected-band analysis further shows that these states are predominantly localized at the central domain-wall region, resembling the interfacial charge localization found in the ZnS/MgS heterostructure.

After full structural relaxation, however, the electronic structure changes qualitatively. As shown by the band structure in Fig. 3(a) and the layer-resolved PDOS in Figs. 3(b) and 3(c), a finite band gap reopens at the Fermi level, converting the metallic unrelaxed domain wall into an insulating one. At the same time, the partial charge densities in Figs. 3(d) and 3(e) show that the residual electronic states remain strongly localized at the domain wall. This indicates that the QFP mismatch is still accommodated locally, but now predominantly through substantial lattice reconstruction rather than metallic screening. The structural distortion is analyzed in detail in the SM. For this system, we retain the PBE functional because the fully relaxed domain wall is already insulating at the PBE level. $HfZnN_2$ thus provides a complementary example in which the QFP mismatch imposes a nontrivial compensation requirement, while structural relaxation selects an insulating reconstruction as the energetically favored response.

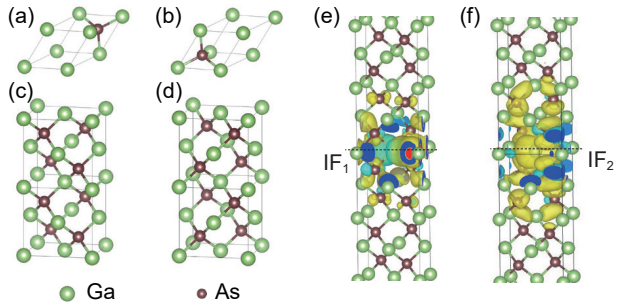

Fig. 4. (a) and (b) Primitive cells of GaAs in the L1 and L2 states, with QFPs of $-1/4$ and $+1/4$, respectively. (c) and (d) Corresponding conventional cells, doubled along the c axis. (e) and (f) Interfacial structures of the GaAs domain wall, showing the stacking sequence of Ga and As atomic layers, together with the electronic states localized near the interfaces.

GaAs provides a particularly revealing test case for the QFP framework, because the interfacial incompatibility is not transparently captured within the conventional formal-polarization picture. GaAs is a zincblende material that crystallizes in the $F\bar{4}3m$ space group with T_d point group symmetry. Through symmetry analysis and first-principles calculations, we find that the primitive cell of GaAs can carry a QFP of $\pm 1/4$ [8]. The two corresponding configurations, denoted as L1 and L2, are related by inversion symmetry and possess opposite QFPs. Their conventional cells, shown in Fig. 4, are displayed for later comparison with the QFP-based analysis.

To make this contrast explicit, we first examine the domain wall using the conventional formal-polarization picture. Following Ref. [19], formal polarization is defined as the sum of the effective (formal) charges multiplied by their position vectors. For this purpose, Ga and As atoms are assigned formal charges of $+Z$ and $-Z$, respectively, although the precise choice of Z does not affect the conclusion. As shown in Figs. 4(c) and 4(d), the conventional cells of L1 and L2 share the same Ga-As-Ga-As stacking sequence, and their formal polarizations are therefore identical within this description. When L1 and L2 are stacked to form the domain wall shown in Fig. 4(e), no obvious polarization discontinuity is apparent at the interface. From this conventional viewpoint alone, one would therefore not naturally anticipate pronounced interfacial effects.

The QFP viewpoint resolves this ambiguity. Although the conventional cells of L1 and L2 appear equivalent from the perspective of formal polarization, their primitive cells carry opposite QFPs, $\pm 1/4$ [8]. When these two states are brought together to form a domain wall, the mismatch between their QFPs signals an intrinsic bulk incompatibility, even though no obvious polarization discontinuity is apparent in the conventional description. The QFP framework therefore predicts that pronounced interfacial effects should nevertheless emerge at the L1/L2 boundary.

To test this prediction, we construct a supercell comprising 10 layers of L1 GaAs and 10 layers of L2 GaAs. The electronic structure of this supercell is evaluated using the HSE hybrid functional to ensure an accurate description of the GaAs band gap and the interface states. As shown in Figs. 4(e) and 4(f), localized electronic states emerge at both interfaces. The corresponding fatband analysis in Fig. 5(a) shows that the bands near the Fermi level are dominated by contributions from atoms adjacent to the interfaces, while the bulk-like states remain gapped. Consistently, the PDOS in Figs. 5(b) and 5(c) shows that atoms located five unit cells away from the interfaces retain a finite band gap characteristic of normal bulk GaAs. These results confirm that metallic interface states emerge at the L1/L2 boundary, consistent with the compensation requirement imposed by the QFP mismatch. This diagnostic advantage of the QFP framework is not unique to GaAs or to the zincblende family. For example, AlBeB also exhibits symmetry-related states with opposite QFPs of $\pm 1/4$, while the corresponding interfacial incompatibility is likewise not transparently

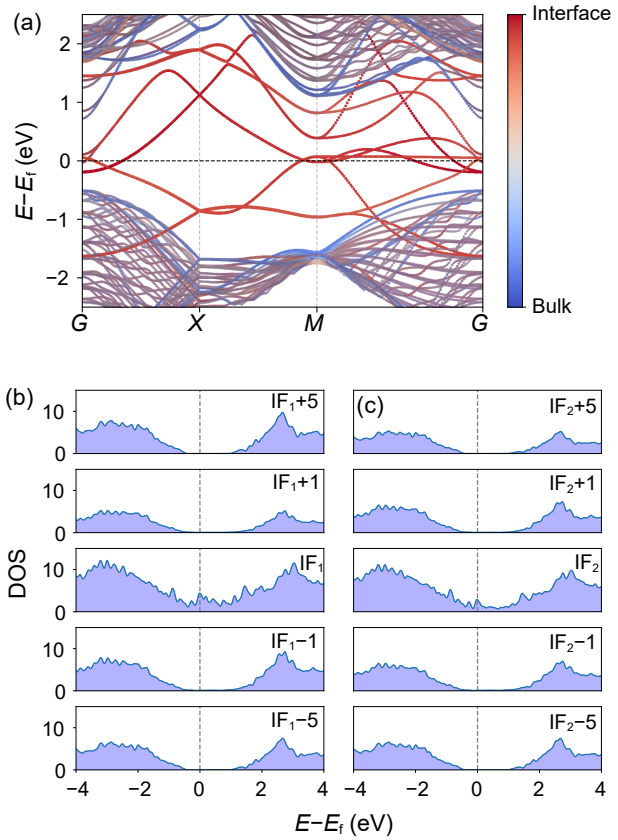

Fig. 5. (a) The fatband of the GaAs superstructure: the red lines represent contributions from atoms near the interface, while the blue lines denote bulk contributions. It is evident that bands near the Fermi level originate exclusively from interfacial atoms. PDOS at different positions relative to interfaces (b) IF_1 and (c) IF_2, demonstrating metallic states at both interfaces.

revealed within the conventional formal-polarization picture. The detailed analysis is presented in the SM.

Conclusion

In conclusion, we establish QFP as a symmetry-protected bulk invariant of crystalline solids. We show that a mismatch between the QFPs of different materials or phases represents a bulk incompatibility and imposes a nontrivial interfacial compensation requirement. This requirement may be realized through different electronic or structural channels, including metallic states, bound-charge redistribution, and structural reconstruction. Because these channels compete energetically, the QFP mismatch alone does not uniquely determine the resulting interfacial state, and explicit interface calculations are generally required to identify the energetically preferred response.

Nevertheless, the QFP framework remains highly useful because the existence of a nontrivial compensation requirement can be diagnosed directly from bulk properties, without first constructing the interface. It therefore provides a predictive bulk criterion for identifying potentially nontrivial interfaces and domain walls, substantially narrowing the space of candidate systems that require detailed interface calculations. In this sense, our work elevates formal polarization from a quantity used mainly in interface electrostatics to a more general bulk principle for diagnosing phase incompatibility and guiding the search for functional interfaces and quantum heterostructures.

Acknowledgements

This work was supported by the Advanced Materials—National Science and Technology Major Project (Grant No. 2025ZD0618401), the Strategic Priority Research Program of Chinese Academy of Sciences (Grant No. XDB0500201), the National Natural Science Foundation of China (Grant No. 12134012), and the Innovation Program for Quantum Science and Technology (Grant No. 2021ZD0301200). The numerical calculations were performed on the USTC HPC facilities.

References

[1] Neumann F E 1885 *Vorlesungen über die Theorie der Elasticität der festen Körper und des Lichtäthers* vol. 5 (B. G. Teubner-Verlag, Leipzig)
[2] Cochran W 1960 *Adv. Phys.* **9** 387
[3] Portengen T, Östreich T, and Sham L 1996 *Phys. Rev. B* **54** 17452
[4] Lines M E and Glass A M 2001 *Principles and Applications of Ferroelectrics and Related Materials* (Oxford, UK: Oxford University Press)
[5] Rabe K M, Ahn C H, and Triscone J M 2007 *Physics of Ferroelectrics: A Modern Perspective* Vol. 105 (Springer Science & Business Media)
[6] Ji J, Yu G, Xu C, and Xiang H 2024 *Nat. Commun.* **15** 135
[7] Yu G, Ji J, Chen Y, Xu C, and Xiang H 2025 *Phys. Rev. Lett.* **134** 016801
[8] Pang H and He L 2025 *Phys. Rev. Lett.* **135** 116402
[9] Vanderbilt D and King-Smith R 1993 *Phys. Rev. B* **48** 4442
[10] Vanderbilt D 2018 *Berry phases in electronic structure theory: electric polarization, orbital magnetization and topological insulators* (Cambridge, UK: Cambridge University Press)
[11] Ohtomo A and Hwang H 2004 *Nature* **427** 423
[12] Nakagawa N, Hwang H Y, and Muller D A 2006 *Nat. Mater.* **5** 204
[13] Savoia A, Paparo D, Perna P *et al.* 2009 *Phys. Rev. B* **80** 075110
[14] Zou K, Ismail-Beigi S, Kisslinger K, Shen X, Su D, Walker F, and Ahn C 2015 *APL Mater.* **3** 036104
[15] Zhang Y, Shen G, Sheng C, Zhang F, and Fan W 2021 *Appl. Surf. Sci.* **562** 150164
[16] Cancellieri C, Fontaine D, Gariglio S *et al.* 2011 *Phys. Rev. Lett.* **107** 056102
[17] Bristowe N, Ghosez P, Littlewood P B, and Artacho E 2014 *J. Phys.: Condens. Matter* **26** 143201
[18] Karmakar S, Kumar G A, Angajala K K, Mistari C D, Amrutha M, Sarkar P K, Taqy S, Chakraborty B, More M, and Haque A 2026 *Sci. Rep.* **16** 16953
[19] Stengel M and Vanderbilt D 2009 *Phys. Rev. B* **80** 241103
[20] Stengel M 2011 *Phys. Rev. B* **84** 205432
[21] Chen M, Guo G C, and He L 2010 *J. Phys.: Condens. Matter* **22** 445501
[22] Li P, Liu X, Chen M, Lin P, Ren X, Lin L, Yang C, and He L 2016 *Comput. Mater. Sci.* **112** 503
[23] Lin P, Ren X, and He L 2021 *Phys. Rev. B* **103** 235131
[24] Lin P, Ren X, Liu X, and He L 2024 *WIREs Comput. Mol. Sci.* **14** e1687
[25] Perdew J P, Burke K, and Ernzerhof M 1996 *Phys. Rev. Lett.* **77** 3865
[26] Heyd J, Scuseria G E, and Ernzerhof M 2003 *J. Chem. Phys.* **118** 8207
[27] Scherpelz P, Govoni M, Hamada I, and Galli G 2016 *J. Chem. Theory Comput.* **12** 3523
[28] King-Smith R D and Vanderbilt D 1993 *Phys. Rev. B* **47** 1651
[29] Jin G, Pang H, Ji Y, Dai Z, and He L 2023 *Comput. Phys. Commun.* **291** 108844
[30] Morkoç H 2009 *Handbook of Nitride Semiconductors and Devices, Materials Properties, Physics and Growth* (John Wiley & Sons)
[31] Resta R and Vanderbilt D 2007 *Theory of polarization: A modern approach, in Physics of Ferroelectrics: A Modern Perspective* (Springer, Berlin, Heidelberg) p. 31